J Solid State Electrochem (2004) 8: 650–654
DOI 10.1007/s10008-004-0506-0

ORIGINAL PAPER

S. Piñol · M. Najib · D. M. Bastidas · A. Calleja
X. G. Capdevila · M. Segarra · F. Espiell
J. C. Ruiz-Morales · D. Marrero-López · P. Nuñez

Microstructure–conductivity relationship in Gd- and Sm-doped ceria-based electrolytes prepared by the acrylamide sol–gel-related method

Published online: 5 March 2004

Abstract We have prepared pure electrolytes of $Ce_{0.8}Gd_{0.2}O_{1.9}$ (CGO) and $Ce_{0.8}Sm_{0.2}O_{1.9}$ (CSO), useful for SOFCs, by a sol–gel-related technique like the acrylamide method. This method consists of preparing a solution from the single oxides followed by gelation. Then, the combustion or decomposition of the organic molecules is initiated, producing nanometric calcined powders of the above-mentioned compounds. Thermal treatments were optimized in order to obtain good electrochemical properties of the electrolytes. We have observed that the synthesis temperature to obtain the pure phase is lower for the sol–gel samples than for the pellets prepared by solid-state reaction, and the final density is higher. The microstructure and composition of the powders were characterized by TEM, SEM, and EDX analysis. The electrical properties of the electrolytes were measured by impedance spectroscopy at different temperatures and oxygen partial pressures.

Keywords SOFC · Ceria · Gd · Sm · Sol–gel · Impedance spectroscopy · Ionic conductivity

Presented at the OSSEP Workshop "Ionic and Mixed Conductors: Methods and Processes", Aveiro, Portugal, 10–12 April 2003

S. Piñol (✉) · M. Najib · D. M. Bastidas
Institut de Ciència de Materials de Barcelona (CSIC),
Campus de la UAB, Bellaterra, E-08193 Barcelona, Spain
E-mail: salva@icmab.es
Tel.: +34-935-801853
Fax: +34-935-805729

A. Calleja · X. G. Capdevila · M. Segarra · F. Espiell
Departament d'Enginyeria Química i Metallurgia,
Facultat de Química, Universitat de Barcelona,
Diagonal 647, E-08028 Barcelona, Spain

J. C. Ruiz-Morales · D. Marrero-López · P. Nuñez
Departamento de Química Inorgánica,
Universidad de La Laguna, E-38200 La Laguna,
Tenerife, Spain

Introduction

The diminishing reserves of petroleum oil and the rising concerns about the environment and global warming have focused attention on the possibility of making more efficient use of H_2, natural gas or higher hydrocarbons, reserves of which are at present considerably underutilized. Using fuel cells as electrical sources, H_2 and methane may be commonly used as fuels and methane can be converted to higher hydrocarbons by Fisher–Tropsch catalysis. So, fuel cells are widely viewed as a promising source of low-cost and low-emission power generation.

There is great controversy over which fuel cells should be used: polymer electrolyte fuel cells (PEFCs) exhibit high power densities at low temperatures (≈75 °C), but they require hydrogen as the fuel, which is very dangerous in terms of storage and handling. On the other hand, there have been successes with solid oxide-based fuel cells (SOFCs), which perform well at high temperature using hydrocarbons directly as the fuel [1, 2, 3, 4]. Nevertheless, a further reduction in the operating temperature of SOFCs and an enhancement in their thermal and mechanical shock resistance would make this technology a promising alternative to PEFCs.

In recent years a new type of SOFC based on doped ceria electrolytes, Ni-based anodes, and perovskite-type cathodes, that consists of only one gas chamber where both the anode and the cathode are exposed to the same mixture of fuel and air, has been reported by some researchers [5, 6]. This type of fuel cell is more shock resistant (both thermally and mechanically) than conventional cells and can achieve sufficient ionic conduction at intermediate temperature (350–450 °C). This one-chamber cell was first prepared from yttria-stabilized zirconia (YSZ), which is commonly used as a solid electrolyte in SOFCs. However, this YSZ-SOFC must operate at the high temperature of ≈1,000 °C to achieve sufficient ionic conduction in the solid electrolyte. In addition, Ni-YSZ cermet anodes are ill suited for the

direct conversion of hydrocarbons at high temperature due to carbon deposition.

Ceria doped with different cations, notably gadolinium-doped ceria (CGO) and samarium-doped ceria (CSO) [7, 8, 9, 10], has much higher ionic conduction than YSZ in an oxidizing atmosphere and may operate at lower temperatures (350–700 °C), at which it becomes a predominantly ionic conductor even in a reducing atmosphere. In addition, a direct electrochemical oxidation of hydrocarbons in the ceria-based electrolytes up to 700 °C has recenty been observed, without any catalyst in the anode [11, 12]. Cu-based anodes were utilized for the direct oxidation of dry hydrocarbon fuels to generate electrical power. This mechanism has the potential to accelerate substantially the use of ceria-based fuel cells in transportation and distributed-power applications [13]. Moreover, SOFCs offer a clean pollution-free technology for the electrochemical generation of electricity with high efficiency [14].

A typical SOFC which utilizes YSZ as electrolyte exhibits an oxide-ion conductivity at 1,000 °C of about 0.1 S cm^{-1}. Lowering the operation temperature would enhance the reliability, lifetime, and operating cost of the cell. This means that a large number of technological and economic benefits are gained such as the use of cheaper interconnector materials, lower degradation problems, and better compatibility of components in terms of thermal expansion coefficient between materials [15]. But, with conventional membranes of YSZ, the reduction in temperature implies poor performance [16]. Alternative to the YSZ, electrolyte materials such as $Ce_{1-x}Ln_xO_{2-(x/2)}$ (Ln = Gd, Sm) [17] are reported to be one of the best candidates for operational temperatures $\leq$ 700 °C. In particular the $Ce_{1-x}Ln_xO_{2-(x/2)}$ ($Ln = Gd^{3+}$, Sm^{3+}) ageing test showed high ionic conductivity ($0.01 < \sigma < 0.075$ S cm^{-1}) between 500 and 800 °C, good chemical stability, negligible electronic conduction over a broad range of oxygen partial pressures, and stable oxide-ion conductivity at 700 °C, for a long time.

Another important aspect for cost and emission reduction of fuel cells is the possibility of using hydrocarbons as fuels. The conventional fuels used in SOFCs are H_2 and/or CO. One of the main technological problems in the hydrogen economy is related to the cost of hydrogen and its storage and/or transportation. Therefore, for the foreseeable future, fuel cells will be supplied with natural gas, which is usually converted to a hydrogen-rich fuel through a steam reforming unit operation (i.e., $CH_4 + H_2O \rightarrow CO + 3H_2$). The reforming process increases the complexity and the cost of the whole device but increases the respect to the environment.

In this work, we propose a low-cost sol–gel method based on gelation by acrylamide for the fabrication of high-purity ceria-doped electrolytes with a nanometric grain size microstructure, which leads to high-density and very pure electrolytes for fuel cell applications with low-cost and low-emission power generation. This method is a quasi-universal medium for the synthesis of nanometric oxide powders for electroceramic applications [18].

Experimental

Powder preparation

We have studied and compared the effect of two different ceramic powder synthesis methods in the preparation of the gadolinium- and samarium-doped ceria-based electrolytes. These methods were: the acrylamide-related sol–gel procedures (AA) and the solid oxide reaction (SS) at high temperature. The powders of CGO and CSO obtained by the AA and solid-state reaction techniques were prepared from single oxides (CeO_2, Gd_2O_3, and Sm_2O_3, 99.9% purity, Aldrich). Stoichiometric quantities of oxide were weighed and dissolved in hot concentrated nitric acid. Then, EDTA was added in order to complex the cations in solution capable of inhibiting AA polymerization. A 1:1 cation-to-EDTA ratio is assumed. The pH was adjusted between 3 and 10 by the addition of an aqueous solution of NH_3. A solution of acrylamide/water (50/50 v/v) was prepared. The volume of this aqueous solution added in each case was calculated taking the whole cation solution volume, determining the mass as if it were pure water, and then adding a 10% v/v of AA with respect to the mass. The resulting solution was heated and the reticulating agent (bisacrylamide or BisAA, 20% with respect to AA) and the polymerization agent (H_2O_2) were introduced. When the solution approached a temperature of 80–90 °C it spontaneously gelled, rendering a consistent gel. The stirring rod was then removed and the drying process initiated by further heating. At first, the gel shrank progressively until the bottom was completely dried. Then the bottom part automatically ignited as a consequence of organic combustion and pyrolysis produced by the presence of nitrates. The resulting xerogels were homogenized in an agate mortar and fired in air in a muffle furnace. Finally, the powders were pressed and sintered at different temperatures up to 1,600 °C.

AC impedance measurements

Powders were uniaxially pressed at 3 MPa for 1 min. The resultant pellets were sintered at 1,500 °C for 10 h (heating and cooling ramp rates were 5 K/min). The relative density calculated by geometry for the sintered pellet was around 94% of the theoretical density. The as-prepared pellets were coated with an organoplatinum paste on each face, dried at 100 °C for 1 h, and fired at 1,000 °C for 15 min.

Electrical measurements were carried out on pellets, using impedance spectroscopy in static air. The pellet was mounted in a "compression jig" with Pt wire electrodes, in a horizontal-tube furnace. The sample was heated up to 1,000 °C at 5 K/min, and impedance measurements were carried out in the temperature range 1,000–200 °C (to resolve bulk and grain boundary processes). Enough time for thermal equilibration and hence reproducible experiments was considered in every step.

Impedance measurements were performed on a Solartron 1260 frequency response analyzer, with AC perturbation of 25 mV in the range 1,000–500 °C and 100 mV for 500–200 °C. Measurements were carried out in the 1 MHz to 1 Hz frequency domain. Typical AC impedance measurements for CGO are shown in Fig. 5.

DC measurements were also performed as a function of the oxygen partial pressure at 1,000 °C, using a potentiostat/galvanostat, Solartron 1287, with the DC four-point method.

Results and discussion

Microstructural characterization

We have prepared high-purity powders of $Ce_{0.8}Gd_{0.2}O_{1.9}$ (CGO) and $Ce_{0.8}Sm_{0.2}O_{1.9}$ (CSO) by the AA sol–gel method and by solid-state reaction as confirmed

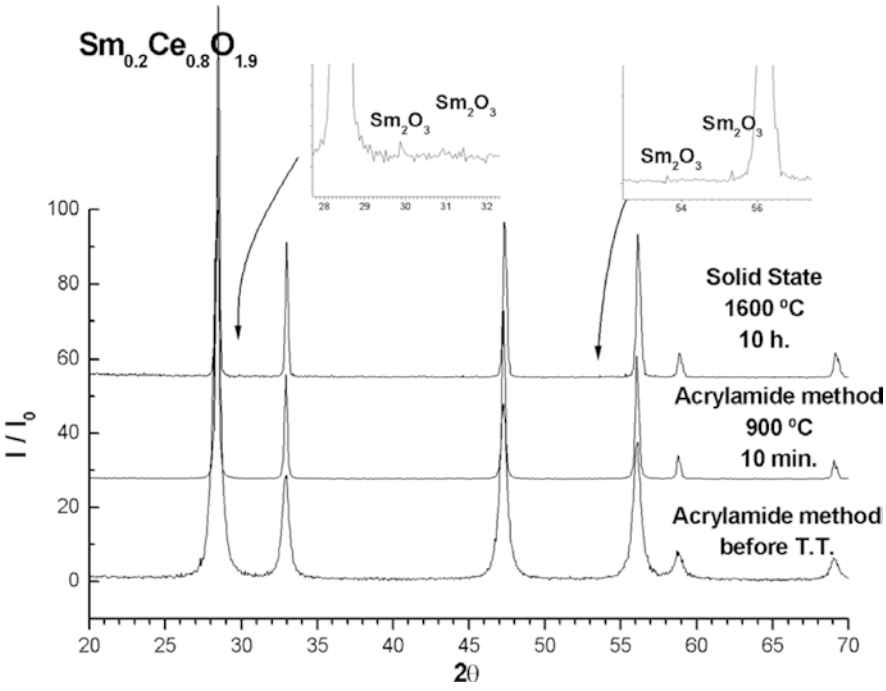

Fig. 1 X-ray diffraction patterns of CSO electrolytes: solid-state reaction of commercial powders heated at 1,600 °C, acrylamide calcined powders at 900 °C, and acrylamide xerogel after combustion

by X-ray diffraction powder analysis. Both techniques give similar purity powders, but the optimal synthesis temperature to obtain a high-purity phase is lower for samples prepared by the AA method. Figure 1 shows the X-ray diffraction pattern of CSO powders prepared by the AA method, before (xerogel) and after calcination at high temperature, and of powders prepared by solid-state reaction. Pellets prepared by the SS method show an unreacted ceria phase even at 1,600 °C. It is very interesting to note that the combustion of the organic polymer at low temperature (~400–500 °C) leads to the formation of a xerogel powder, which is almost a single CSO phase. The density of pellets prepared from the xerogel obtained by the AA method increases drastically with temperature, reaching 94% of the theoretical density at temperatures as high as 1,500 °C, while the highest density of pellets prepared by the solid-state procedure is ~92% (see Fig. 2). Optical microscopy was used to determine the grain size distribution in the AA sintered pellets; the grain size diameter may attain a few microns (10–20 μm) after heat treatment at high temperature (1,600 °C) for 10 h. A SEM microphotograph of the CGO grain structure for a pellet prepared by the AA method at 1,600 °C is presented in Fig. 3. The microstructure of powders was also examined by TEM microscopy (see Fig. 4); the analysis of the powders prepared by AA sol–gel techniques shows a porous foamy microstructure. Applying Scherrer's formula to the xerogel one obtains a crystallite size of 30 nm. This nanometric size of CGO and CSO particles is responsible for the enhanced sintering reactivity at lower temperatures compared to the solid-state reacted samples. The TEM micrograph of calcined powders of CGO and CSO shows a narrow particle size distribution around 0.5 μm.

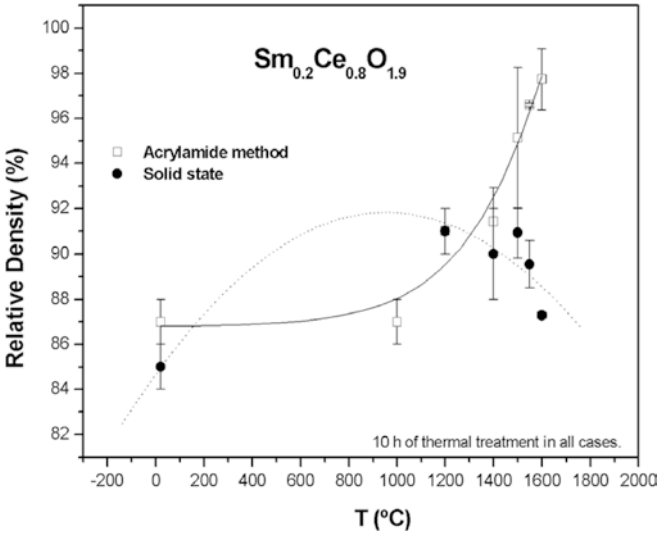

Fig. 2 Relative density plot as a function of temperature for CSO prepared by the acrylamide and solid-state reaction methods at different temperatures

Electrical characterization

The impedance spectrum for CGO pellets (Fig. 5) shows two well-resolved arcs, which may be ascribed to the bulk (grain interiors) and grain boundary. Equivalent circuits formed by a series association of (R_i–CPE_i), R_i being a resistance contribution and CPE_i a pseudo capacitance, were used to fit impedance data. The analysis was performed with the program ZPLOT v2.2 from Scribner.

The conductivity $\sigma = L/(A \cdot R)$ was obtained taking into account the thickness to area ratio L/A and resistance R of the different contributions. The temperature

dependence of total conductivity (bulk and grain boundary) was plotted using the Arrhenius equation:

$$\sigma = \frac{\sigma_0}{T} \cdot e^{-\frac{E_A}{kT}}$$

where σ_0 is a constant that contains the jump attempt frequency and distance, the concentration and mobility of the ionic charge carriers, and a geometrical factor; E_A is the activation energy.

The Arrhenius plot for the total conductivity (Fig. 6) shows two behaviors with different activation energies. Below 700 °C the activation energy is about 1.0 eV, however at higher temperature there is a slope change and the activation energy decreases. This change is probably due to the increasing interactions between the charge carriers and the dopant Gd^{3+} [19].

From the equivalent circuit fitted, we can discriminate between the bulk and grain boundary resistances. The corresponding Arrhenius plots of the bulk and grain boundary are shown in Fig. 7; the activation energies are 0.86 and 1.05 eV, respectively. These values are in agreement with previous works [20, 21].

A DC four-terminal configuration was used to study the isothermal conductivity at 1,000 °C at different oxygen partial pressures. A constant flow of 5% H_2/Ar was introduced into the cell for 5 h, and measurements were made during the reoxidation process (Fig. 8). The total conductivity of the sample in reducing conditions is described by the power law $(Po_2)^{-1/n}$ supposing that n-type conductivity is predominant [22]:

$$\sigma_{\text{total}} = \sigma_{\text{ionic}} + \sigma_{\text{n-type}} = \sigma_{\text{ionic}} + m \cdot p(O_2)^{-1/n}$$

where n takes values in the range 4 to 6.

At low Po_2, the conductivity increases as a function of $p(O_2)^{-1/6}$ indicating n-type conductivity as the dominant electronic mechanism due to partial reduction of Ce^{4+} to Ce^{3+}. We have also performed impedance measurements on CSO, however the observed conduc-

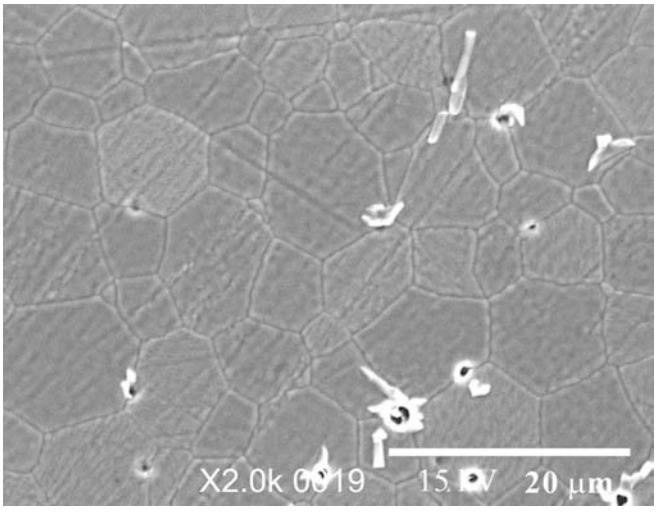

Fig. 3 SEM microphotograph of a CGO pellet prepared from powders obtained by the acrylamide sol–gel method after pressing at ca. 800 MPa and sintering at 1,600 °C for 10 h

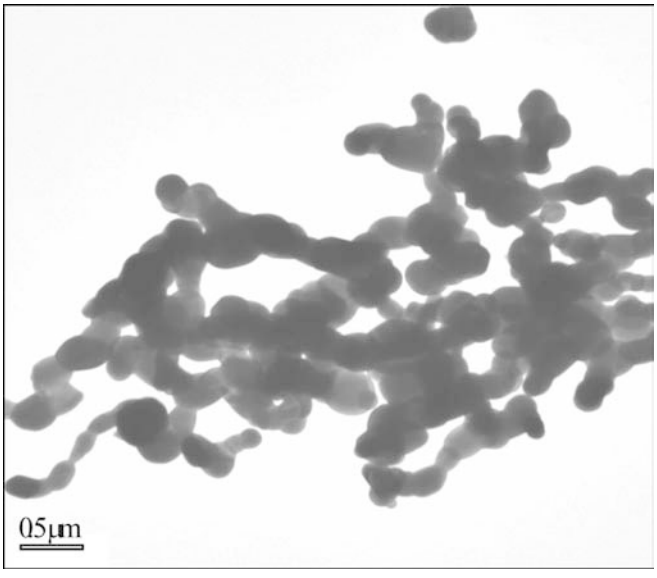

Fig. 4 TEM microphotograph of CGO powder calcined at 1,000 °C for 2 h

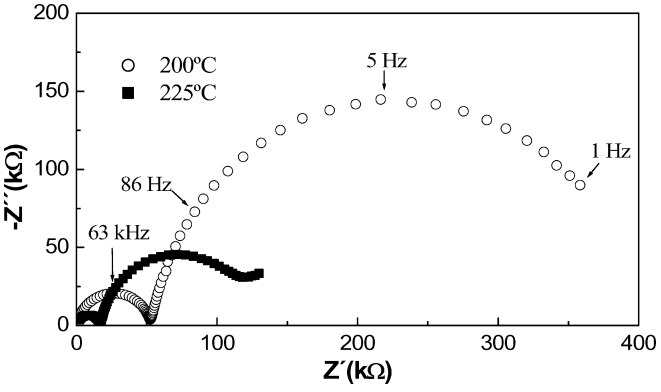

Fig. 5 Impedance spectra for $Ce_{0.8}Gd_{0.2}O_{1.9}$ at 200 and 225 °C

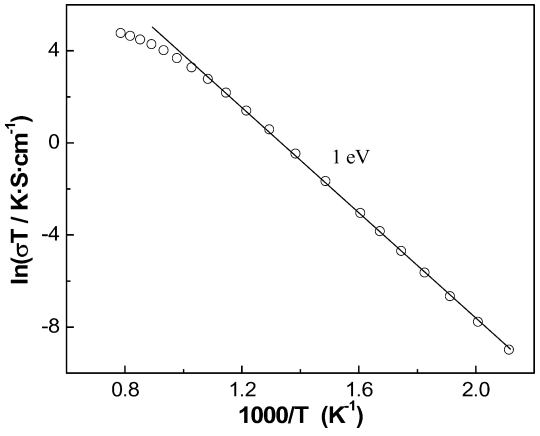

Fig. 6 Arrhenius plot of total conductivity for $Ce_{0.8}Gd_{0.2}O_{1.9}$, in air, on cooling from 1,000 to 200 °C

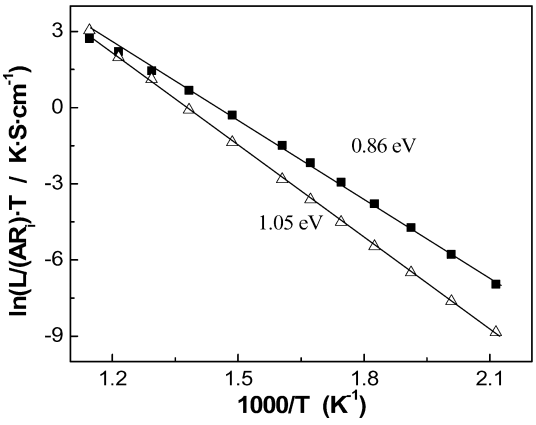

Fig. 7 Arrhenius plot of bulk (*full squares*) and grain boundary (*open triangles*) results in static air for samples of $Ce_{0.8}Gd_{0.2}O_{1.9}$ sintered at 1,500 °C for 10 h

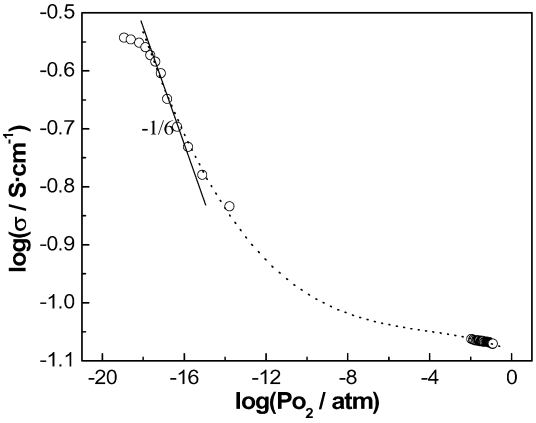

Fig. 8 Electrical conductivity vs. partial pressure of O_2, measured on slow reoxidation after equilibration in 5% H_2/95% Ar, for $Ce_{0.8}Gd_{0.2}O_{1.9}$ at 1,000 °C

tivity was lower than the values reported in the literature. Different preparations changing the reaction conditions were examined, but similar electrical results were obtained for CSO. We associate this anomaly with impurity traces from the solvent, that in the case of the samarium compound remain in the final phase.

Conclusions

The acrylamide (AA) sol–gel technique is a useful process for obtaining nanocrystalline powders of CGO and CSO at lower sintering temperatures than with the solid-state reaction method. By the AA sol–gel method, it is possible to obtain very-high-density electrolytes (~94% of theoretical density) of CGO when compared with samples from the solid-state reaction. This higher density is due to the resulting nanometric grain size of the precursors after the combustion of the organic polymer, this method being interesting in view of cost-effective ceramic processing of SOFC. Impedance spectroscopy analysis of CGO and CSO obtained by the acrylamide sol–gel-related method reveals a better conductivity for CGO than for CSO samples. Probably, impurities from solvents and reagents play a most important negative role in CSO samples.

Acknowledgements The authors are grateful to the Spain–Portugal project HP01-82 and to Prof. J.R. Frade for his helpful comments.

References

1. Minh NQ, Takahashi T (1995) Science and technology of ceramic fuel cells. Elsevier, New York
2. Milliken C, Guruswamy S, Khandkar A (1999) J Electrochem Soc 146:872
3. Eguchi K, Setoguchi T, Inoue T, Aria H (1992) Solid State Ionics 52:165
4. Singhal SC (2000) Solid State Ionics 135:305
5. Hibino T, Hasimoto A, Inoue T, Tokuno J, Yoshida S, Sano M (2000) Science 288:2031
6. Hibino T, Wang S, Kakimoto S, Sano M (1999) Electrochem Solid-State Lett 2:317
7. Steele BCH (2000) Solid State Ionics 129:95
8. Huijsmans JPP (2001) Curr Opin Solid St Mater 5:317
9. Yamamoto O (2000) Electrochim Acta 5:2423
10. Kleinlogel C, Gauckler LJ (1999) In: Singhal SC, Dokiya M (eds) SOFC-V. Electrochemical Society, Pennington, 99–119:225
11. Park S, Vohs JM, Gorte RJ (2000) Nature 404:265
12. Park S, Vohs JM, Gorte RJ (1999) J Electrochem Soc 146:3603
13. Steele BCH (1999) Nature 400:620
14. Riley B (1990) J Power Sources 29:223
15. Minh NQ (1993) J Am Ceram Soc 76:563
16. Vlasov AN, Perfiliev MV (1987) Solid State Ionics 25:245
17. Steele BCH (2001) J Mater Sci 36:1053
18. Sin A, Odier P (2000) Adv Mater 12(9):649
19. Huang K, Feng M, Goodenough JB (1998) J Am Ceram Soc 81:357
20. Pérez-Coll D, Nuñez P, Frade JR, Abrantes JCC (2004) Electrochim Acta (in press)
21. Fagg DP, Abrantes JCC, Pérez-Coll D, Nuñez P, Kharton VV, Frade JR (2003) Electrochim Acta 48:1023
22. Navarro L, Marques F, Frade J (1997) J Electrochem Soc 144:267